# Superconducting tunable filter with constant bandwidth using coplanar waveguide resonators*

Ying Jiang(蒋莹)[1], Bo Li(李博)[2], Bin Wei(魏斌)[1,†],
Xu-Bo Guo(郭旭波)[1], Bi-Song Cao(曹必松)[1], and Li-Nan Jiang(姜立楠)[1]

[1] *State Key Laboratory of Low-Dimensional Quantum Physics, Department of Physics, Tsinghua University, Beijing* 100084, *China*
[2] *Department of Electronic Engineering, Tsinghua University, Beijing* 100084, *China*

(Received 17 May 2017; revised manuscript received 19 June 2017; published online 20 August 2017)

In this paper we propose a two-pole varactor-tuned superconducting filter using coplanar waveguide (CPW) spiral-in-spiral-out (SISO) resonators. Novel internal and external coupling structures are introduced to meet the requirements for a tunable filter with a constant absolute bandwidth. The fabricated device has a frequency tuning range of 14.4% at frequencies ranging from 274.1 MHz to 317.7 MHz, a 3-dB bandwidth of $5.14 \pm 0.06$ MHz, and an insertion loss of 0.08 dB–0.70 dB. The simulated and measured results are in excellent agreement with each other.

**Keywords:** coplanar waveguide (CPW), superconducting, tunable filter, varactor

**PACS:** 85.25.–j **DOI:** 10.1088/1674-1056/26/10/108501

## 1. Introduction

Filters are playing important roles in the present modern wireless communication systems. A series of filters has been investigated for decades.[1,2] Filters have been applied to space communication,[3,4] gas detecting,[5] filtering the noises,[6] laser devices,[7,8] optical devices,[9,10] and some other areas.[11,12] Tunable filters have received much attention due to their increasing importance in improving the flexibilities of current and future wireless communication systems.[13–18] Superconducting tunable filters with the advantages of low insertion loss, steep band-edge, and high out-of-band rejection are attractive for these applications.[19–22] A tunable filter is generally required to possess a constant absolute bandwidth with the tunable center frequency. Various design methods have been proposed, such as stepped impedance resonator,[23] coupling reducer or line,[24,25] independent electric and magnetic coupling scheme[26,27] mixed electric and magnetic coupling scheme,[28,29] and extra loaded tuning components.[30] Most of these filters operate at frequencies above 500 MHz. Research at lower frequencies is still scarce until now. Resonators at low frequencies are generally spiraled for size miniaturization and the coupling structures are very complex.[31] Moreover, improving the tuning range is also difficult because the tuning range generally decreases as frequency decreases.

In this paper, novel coplanar waveguide (CPW) spiral-in-spiral-out (SISO) resonators and internal and external coupling structures are proposed to implement a tunable filter at 300 MHz. A compact superconducting tunable filter with a wide tuning range of 14.4% is demonstrated. Measurements show a low insertion loss and an almost constant bandwidth without using any tuning components.

## 2. Filter design procedure

### 2.1. Resonator topology

The microstrip SISO resonator structure in Fig. 1(a) has the advantages of compact size and easy to load tuning element. One end of the resonator is shorted to the grounding pad, and the other end is loaded with a varactor diode. A chip capacitor is added between the varactor and ground as a direct current (DC) block. Assuming that the inductance of the resonator is constant, the tuning range of the resonator can be expressed as[21]

$$\frac{\Delta f}{f_0} = -\frac{\Delta C}{2C}, \tag{1}$$

where $f_0$ and $\Delta f$ are the resonant frequency and tuning range, respectively, $C$ is the equivalent lumped-element capacitor of the resonator, and $\Delta C$ is the capacitance tuning range of the varactor diode. The parallel plate capacitance between the microstrip line and the ground on the back side of the substrate is quite large, which limits the tuning range of the microstrip SISO resonator.

The coplanar waveguide (CPW) and microstrip line are most widely used planar quasi-TEM mode transmission lines. CPW was first proposed in Ref. [32]. The CPW can be easily integrated with lump elements without via-hole grounding. Using the CPW is suitable for connecting a quarter-

*Project supported by the National Natural Science Foundation of China (Grant No. 61371009) and the National High Technology Research and Development Program of China (Grant No. 2014AA032703).

†Corresponding author. E-mail: weibin@mail.tsinghua.edu.cn

© 2017 Chinese Physical Society and IOP Publishing Ltd 

wavelength resonator to the ground, integrating tunable components, and adding voltage. The proposed CPW SISO resonator is shown in Fig. 1(b). The signal line and ground are on the same side of the substrate, thus eliminating the parallel plate capacitance in the microstrip structure. As a result, the tuning range can be significantly improved. A comparison of the two resonator structures simulated by Sonnet EM software is shown in Table 1. A 0.5-mm thick MgO substrate with a relative dielectric constant of 9.7 and a loss tangent of $5.5 \times 10^{-6}$ is used. The capacitance of the varactor changes from 1.1 pF to 0.2 pF. The capacitance of the CPW SISO resonator is reduced by half, whereas the tuning range is increased to 14.4%.

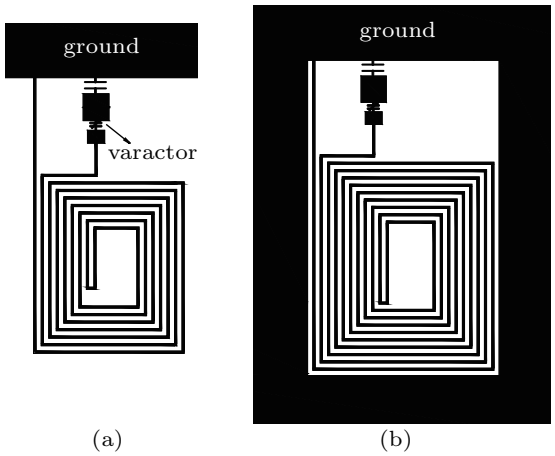



**Fig. 1.** (a) Microstrip SISO resonator; (b) proposed CPW SISO resonator (not to be scaled).

**Table 1.** Comparison of different resonator structures.

| Resonator structure | $f_0$/MHz | $\Delta f$/MHz | Tuning range | Estimated $C$/pF |
|---|---|---|---|---|
| Microstrip SISO | 298.05 | 22.8 | 7.6% | 5.92 |
| CPW SISO | 296.95 | 42.9 | 14.4% | 3.12 |

The wideband resonance response from 100 MHz to 1000 MHz of the CPW SISO is shown in Fig. 2. The first spurious resonance is at about twice the center frequency. There are no other spurious resonances occurring, that is to say, no ground resonance is excited.

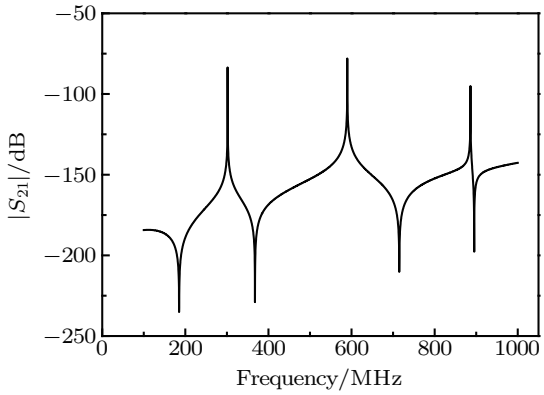



**Fig. 2.** Wideband response of CPW SISO.

### 2.2. Coupling coefficient

According to Ref. [33], for a second-order Chebyshev filter, the required coupling coefficient $k_{12}$ can be calculated from the following equation

$$k_{12} = \frac{BW}{f_0\sqrt{g_1 g_2}}, \tag{2}$$

where $BW$ represents the absolute bandwidth, $f_0$ is the center frequency, and $g_i$ is the element value of the low-pass prototype filter. The coupling coefficient should vary inversely with the tuning frequency to maintain a constant absolute bandwidth.

Table 2 shows 2-pole tunable coupling coefficients and external $Q$-factor when the center frequency varies from 276.25 MHz to 319.09 MHz, and the 3-dB bandwidth is 5.2 MHz.

**Table 2.** Design specifications for a tunable filter with constant bandwidth.

| Center frequency/MHz | 276.25 | 290.53 | 304.81 | 319.09 |
|---|---|---|---|---|
| $k_{12}$ | 0.01307 | 0.01243 | 0.01185 | 0.01132 |
| $Q$ | 75.693 | 76.336 | 78.682 | 83.899 |

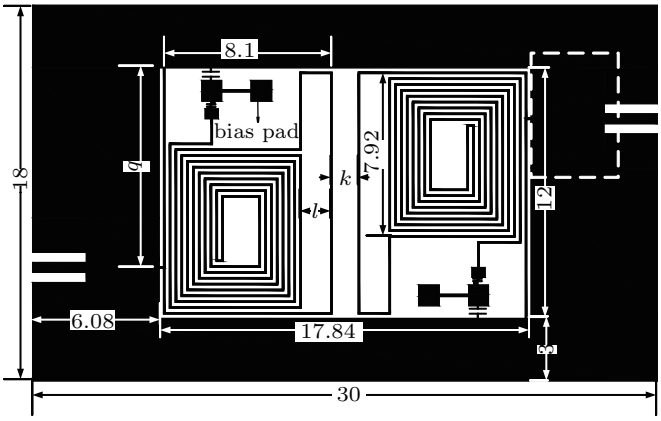



**Fig. 3.** Layout of two-pole tunable filter.

The proposed coupling scheme for $k_{12}$ is a parallel-coupled line structure near the shorted ends of the two resonators as shown in Fig. 3. The coupling property is mainly magnetic. Electromagnetic simulations show that the coupling coefficient decreases with frequency increasing as shown in Fig. 4. The slope of $k_{12}$ can be changed by the gap between the outer line and the inner spiral of the resonator, $l$. The slope becomes steeper as $l$ is increased. Moreover, the strength of coupling is affected by the coupling gap between the two resonators, $k$. Finally, coupling parameters $l = 1.4$ mm and $k = 1.24$ mm for the coupling $k_{12}$ are selected. The simulated coupling strength shows a deviation of less than 0.0003 from the desired coupling coefficient, which will result in a 1% bandwidth deviation.

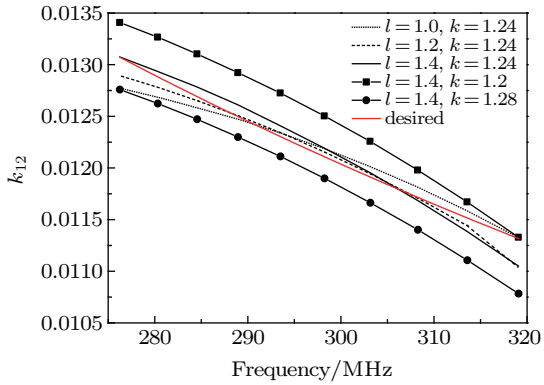



**Fig. 4.** (color online) Variations of simulated coupling coefficient $k_{12}$ with resonance frequency for different values of $l$ and $k$. The dashed line represents the desired results calculated from Eq. (2).

### 2.3. External $Q$

Interdigital capacitors are introduced between the feedlines and grounding pads as inverters. The interdigital capacitors in the external coupling structure are shown in detail in Fig. 5. The external coupling lines are taped to the resonator with a tap position $q$.

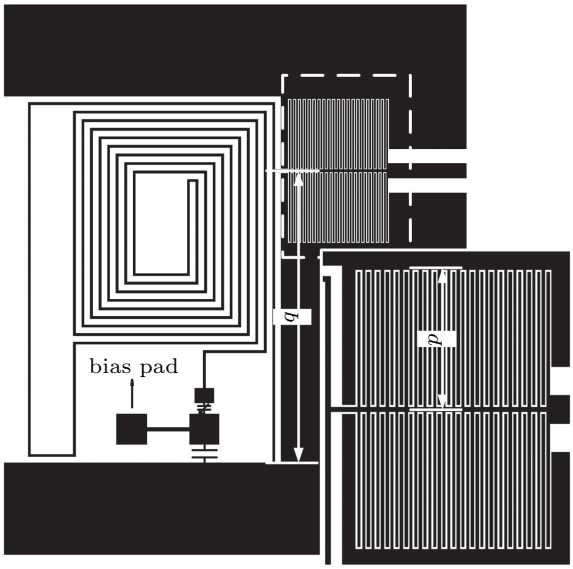



**Fig. 5.** Detailed external coupling topology.

Interdigital capacitors are widely used as quasi-planar lumped components[34] as shown in Fig. 6. When the width of the interdigital finger, $W$, equals the distance between interdigital fingers, $s$, the largest capacitance density can be obtained. Assuming that the thickness of the substrate is much larger than the width of the interdigital finger, the capacitance between the interdigital fingers can be calculated from[35]

$$C = 3.937 \times 10^{-5} p(\varepsilon_r + 1)[0.11(n-3) + 0.252] \quad \text{(pF)}, \quad (3)$$

where $\varepsilon_r = 9.7$ is the relative dielectric constant of the substrate, $p$ is the length of the interdigital finger, and $n$ is the number of interdigital fingers.

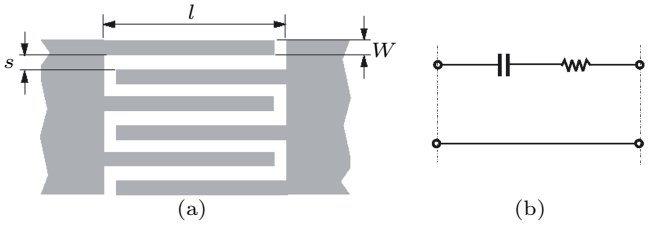



**Fig. 6.** (a) Structure of interdigital capacitor (b) equivalent circuit of interdigital capacitor.

The external $Q$ for the two-pole filter is given by[33]

$$Q_e = \frac{g_0 g_1 f_0}{BW}. \quad (4)$$

The $Q_e$ should increase linearly with frequency to achieve a constant bandwidth. Lumped inductors or capacitors are usually introduced into input/output coupling structures to control $Q_e$.[23,25] However, these will either introduce extra loss or increase the design complexity.

According to Eq. (3), the length of interdigital capacitor, p, determines the capacitance value. The simulations in Fig. 7 show that both $p$ and $q$ can affect $Q_e$. By properly selecting these two parameters ($p = 2.12$ mm and $q = 11.84$ mm), the desired $Q_e$ is almost obtained within the entire frequency tuning range. The largest difference between the simulated $Q_e$ and the desired one is 1.7 which leads to a 0.3% bandwidth deviation. Therefore, a good passband shape can be obtained in the entire tuning range. This external coupling structure benefits the tunable filter with a compact size and low loss.

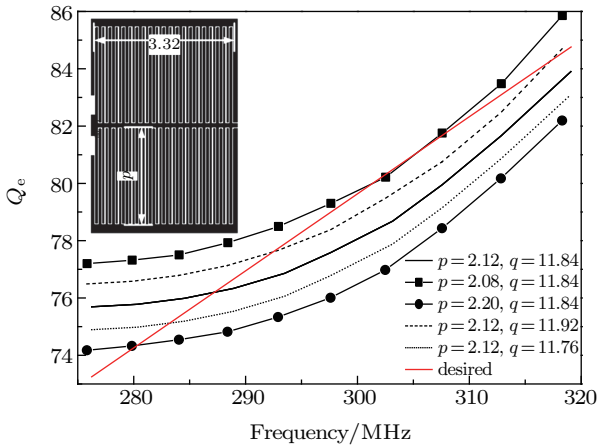



**Fig. 7.** (color online) Variations of simulated $Q_e$ with frequency for different values of $p$ and $q$. The inset shows the detail of interdigital capacitor.

### 2.4. Filter design

A two-pole tunable filter with a constant bandwidth is designed as illustrated in Fig. 3. The filter has a compact size of 30 mm×18 mm. The linewidth of the resonator is 0.08 mm. The linewidth and gaps of the interdigital capacitors are both 0.04 mm. The simulated results are shown in Fig. 8. The filter has a tuning range of 275.5 MHz–318.4 MHz and a 3-dB bandwidth of 5.17 MHz with a deviation of less than 1.0%.

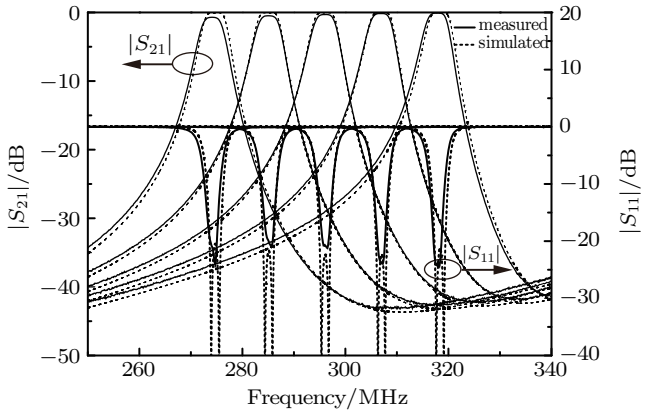



**Fig. 8.** Simulated and measured *S*-parameters of the HTS tunable filter.

## 3. Fabrication and measurement

The tunable filter is fabricated with double-sided YBCO films on an MgO substrate with a thickness of 0.5 mm. CPW has a single layer structure. The bottom metal is etched and only retains a metal ring around the substrate, and the circuit is hung in the air with a cavity under the circuit, drilled in the metal shield box. Varactors (M/A-COM MA46H120) and 100-nF DC block capacitors (ATC 550L104KTT) with high *Q*-factor and small size are surface-mounted into the circuit with silver epoxy glue. The DC bias for each varactor is applied to the circuit via a feed-through capacitor. The varactor changes from 1.1 pF to 0.2 pF with a bias voltage in a range from 0 V to 13.9 V. The *S*-parameters of the filter are measured with an Agilent N5230A Network Analyzer at 70 K. The obtained values are in agreement with the simulation results as shown in Fig. 8. The measured results with different bias voltages are shown in Table 3. The experimental tuning range is 14.4% (from 274.1 MHz to 317.7 MHz) with a 3-dB bandwidth of $5.14 \pm 0.06$ MHz. The insertion losses range from 0.08 dB to 0.70 dB, thus yielding the values of $Q_{\mathrm{u}}$ ranging from 1000 to 11000. The return loss is better than 20 dB. The measured input third-order intermodulation intercept point (IIP3) is approximately 12 dBm for 1-MHz frequency spacing at 296 MHz. A comparison between this device and other tunable filters in Refs. [25]–[30] is presented in Table 4. The proposed filter shows less bandwidth deviation and lower insertion loss than the other filters.

**Table 3.** Measured results of the fabricated device.

| No. | Bias voltage/V | Frequency /MHz | Bandwidth /MHz | Insertion loss/dB | Estimated Resonator *Q* |
|---|---|---|---|---|---|
| 1 | 0 | 274.11 | 5.10 | 0.70 | 1000 |
| 2 | 1.0 | 285.04 | 5.20 | 0.48 | 1500 |
| 3 | 2.1 | 295.97 | 5.19 | 0.30 | 2500 |
| 4 | 4.4 | 306.76 | 5.16 | 0.16 | 5000 |
| 5 | 13.9 | 317.67 | 5.07 | 0.08 | 11000 |

**Table 4.** Comparison between this work and related research.

| Ref. | Filter order | Tuning range/MHz | *C*/pF | Insertion loss/dB | Bandwidth/MH |
|---|---|---|---|---|---|
| [25] | 2, HTS | 924.5–1030.8 | 0.2–1.1 | 0.2–1.4 | 23.8±0.3 |
| [26] | 2 | 800–1335 | 0.9–5.1 | 1.9–2.9 | 43±3 |
| [27] | 2 | 1320–1890 | 0.5–2 | 2.5–2.92 | 70±4 |
| [28] | 2 | 680–1000 | 2–4.5 | 1.2–1.5 | 80±3.5 |
| [29] | 2 | 1700–2200 | 0.67–2 | 1.6–2.0 | 98±7 |
| [30] | 3 | 2250–2555 | 0.63–2.67 | 2.4–3.78 | 189.2±6 |
| This work | 2, HTS | 274.1–317.7 | 0.2–1.1 | 0.08–0.7 | 5.14±0.06 |

## 4. Conclusions

A tunable HTS filter with low insertion loss and a constant absolute bandwidth is proposed. Analysis, design, and experiments of the filter are presented, showing that the coupling coefficient deviation is controlled to obtain a constant bandwidth. The measured results show a tuning range of 14.4% in a frequency range from 274.1 MHz to 317.7 MHz and a 3-dB bandwidth of 5.14 MHz with a deviation of only 1.2%. Meanwhile, the filter is very compact.

## References

[1] Zeng Z, Yao Y and Zhuang Y 2015 *Acta Phys. Sin.* **64** 164101 (in Chinese)
[2] Zhang Q S, Zhu F J and Zhou H M 2015 *Chin. Phys. B* **24** 107506
[3] Xu J, Hong W, Zhang H and Tang H 2017 *IEEE Microw. Wireless Compon. Lett.* **27** 251
[4] Sekiya N 2015 *IEEE Trans. Appl. Supercond.* **25** 1501004
[5] Li Y L, Yang B C and Xu X M 2016 *Chin. Phys. B* **25** 024208
[6] Cao D Y, Liu B H, Wang Z, Huang Y F, Li C F and Guo G C 2015 *Sci. Bull.* **60** 1128
[7] Lin J, Xu Y, Fang Z, Wang M, Wang N, Qiao L, Fang W and Cheng Y 2015 *Sci. China-Phys. Mech. Astron.* **58** 114209
[8] Li X 2015 *Sci. Bull.* **60** 1045
[9] Long H, Huang Y Z, Yang Y D, Zou L X, Xiao J L and Xiao Z X 2015 *Sci. China-Phys. Mech. Astron.* **58** 114205
[10] Gan L and Li Z Y 2015 *Sci. China-Phys. Mech. Astron.* **58** 114203
[11] Wang J J, Glesk I and Chen L R 2016 *Sci. Bull.* **61** 879
[12] Wang L, Lin X W, Hu W, Shao G H, Chen P, Liang L J, Jin B B, Wu P H, Qian H, Lu Y N, Liang X, Zheng Z G and Lu Y Q 2015 *Light-Sci. Appl.* **4** e253
[13] Nguyen P H, Grewe A, Fesser P, Seifert A, Sinzinger S and Zappe H 2016 *Light-Sci. Appl.* **5** e16058
[14] Li X H, Zhou H M, Zhang Q S and Hu W W 2016 *Chin. Phys. B* **25** 117505
[15] Wang X, Deng Y, Wang W-T, Yuan H Q, Bai J H and Liu Y 2016 *Chin. Phys. Lett.* **33** 104202

[16] Wang J H, Chen C M, Zheng Y, Wang X B, Yi Y J, Sun X Q, Wang F and Zhang D M 2017 *Chin. Phys. B* **26** 024212
[17] Xu E M, Zhang Z X and Li L 2017 *Chin. Phys. Lett.* **34** 014203
[18] Deng L, Li D, Liu Z, Meng Y, Guo X and Tian Y 2017 *Chin. Phys. B* **26** 024209
[19] Prophet E M, Musolf J, Zuck B F, Jimenez S, Kihlstrom K E and Willemsen B M A 2005 *IEEE Trans. Appl. Supercond.* **15** 956
[20] Park S J, El-Tanani M A, Reines I and Rebeiz G M 2008 *IEEE Trans. Microw. Theory Techniq.* **56** 2348
[21] Ying Z J, Wei B, Cao B S, Guo X B, Zhang X P, Zhang G Y, Li Q R and Feng C 2013 *IEEE Microw. Wireless Compon. Lett.* **23** 19
[22] Suo G N, Guo X B, Cao B S, Wei B, Zhang X P, Shang Z J and Zhang G Y 2014 *IEEE Microw. Wireless Compon. Lett.* **24** 170
[23] Kim B W and Yun S W 2004 *IEEE Trans. Microw. Theory Techniq.* **52** 1279
[24] Sanchez-Renedo M, Gomez-Garcia R, Alonso J I and Briso-Rodriguez C 2005 *IEEE Trans. Microw. Theory Techniq.* **53** 191
[25] Suo G N, Guo X B, Cao B S, Wei B, Zhang X P, Zheng T N and Zhang G Y 2014 *IEEE Microw. Wireless Compon. Lett.* **24** 628
[26] Park S J and Rebeiz G M 2008 *IEEE Trans. Microw. Theory Techniq.* **56** 1137
[27] El-Tanani M A and Rebeiz G M 2010 *IEEE Trans. Microw. Theory Techniq.* **58** 956
[28] Zhang X Y, Xue Q, Chan C H and Hu B J 2010 *IEEE Trans. Microw. Theory Techniq.* **58** 1557
[29] Wang X G, Cho Y H and Yun S W 2012 *IEEE Trans. Microw. Theory Techniq.* **60** 1569
[30] Xiang Q Y, Feng Q Y, Huang X G and Jia D H 2013 *IEEE Trans. Microw. Theory Techniq.* **61** 1124
[31] Zhang Y, Guo X B, Cao B S, Wei B, Zhang X P, Song X K, Suo G N and Zhang G Y 2012 *IEEE Trans. Appl. Supercond.* **22** 1500205
[32] Wen C P 1969 *IEEE Trans. Microw. Theory Techniq.* **17** 1087
[33] Hong J S 2011 *Microstrip Filters for RF/Microwave Applications*, 2nd edn. (New York: Wiley)
[34] Wang J C, Wei B, Cao B S, Zhang X P, Guo X B and Song X K 2013 *IEEE Trans. Appl. Supercond.* **23** 1502108
[35] Alley G D 1970 *IEEE Trans. Microw. Theory Techniq.* **18** 1028